Journal of the European Ceramic Society **14** (1994) 295–302

Preparation and Characterization of Mullite–Zirconia Composites from Various Starting Materials

Toshiyuki Koyama, Shigeo Hayashi, Atsuo Yasumori & Kiyoshi Okada

Department of Inorganic Materials, Tokyo Institute of Technology,
O-Okayama 2-12-1, Meguro-ku, Tokyo, Japan

(Received 30 November 1993; revised version received 1 March 1994; accepted 5 May 1994)

Abstract

Mullite–zirconia composites were prepared from three kinds of combination of starting materials such as mullite–zirconia (MM), alumina–silica–zirconia (RS3) and alumina–zircon (RS2). Phase formation reaction, sinterability and microstructures of these samples were investigated. Sinterability was good in all the samples and they reached almost full density by firing at around 1520°C. The microstructure of the MM sample was composed of two different types of mullite grains, which were elongated large grains and equiaxed small grains, and intergranularly dispersed zirconia grains. That of the RS3 sample was composed of only equiaxed mullite grains and intergranularly dispersed zirconia grains whereas that of the RS2 sample was composed of irregularly shaped mullite grains and round-shaped zirconia grains, which were distributed intragranularly and intergranularly. The chemical composition of mullite was examined from the length of the lattice parameter of the a-axis. Only mullite in the RS2 samples was found to be apparently richer than 60 mol% in alumina composition, but it approached to 60 mol% Al_2O_3 by annealing at 1570°C.

Mullit–Zirkoniumdioxid-Verbunde wurden aus drei verschiedenen Ausgangskombinationen, wie, z.B. Mullit–Zirkoniumdioxid (MM), Aluminiumoxid–Siliziumdioxid–Zirkoniumdioxid (RS3) und Aluminium–Zirkon (RS2) hergestellt. Die Phasenbildungsreaktionen, die Sinterfähigkeit und das Mikrogefüge dieser Proben wurde untersucht. Die Sinterfähigkeit aller Proben war gut und es konnte nahezu volle Dichte erzielt werden, wenn die Proben bei etwa 1520°C gefeuert wurden. Das Mikrogefüge der MM-Proben bestand aus zwei verschiedenen Mullitkorntypen: gestreckten großen Körnern und gleichachsigen, kleinen Körnern und aus intergranular verteilten Zirkoniumdioxidkörnern. Das Gefüge der RS3-Proben setzte sich aus gleichachsigen Mullit- und intergranular verteilten Zirkoniumdioxidkörnern zusammen, während das RS2-Probengefüge aus unregelmäßig geformten Mullit- und runden Zirkoniumdioxidkörnern bestand, die intergranular und intragranular verteilt waren. Die chemische Zusammensetzung des Mullits wurde mittels der Abmessung des Gitterparameters der a-Achse untersucht. Nur der Mullit in den RS2-Proben zeigte offensichtlich einen Aluminiumoxid-anteil größer als 60 mol%, der sich jedoch 60 mol% näherte, wenn die Proben bei 1570°C angelassen wurden.

Des composites mullite–zircone ont été préparés au départ de trois combinaisons différentes de matières premières : mullite–zircone (MM), alumine–silice–zircone (RS3) et alumine–zircon (RS2). Les réactions de formation des phases, l'aptitude au frittage et les microstructures de ces échantillons ont été examinés. L'aptitude au frittage de tous les échantillons est bonne et ils atteignent presque la densité théorique par un traitement thermique à 1520°C. La microstructure de l'échantillon MM est composée de deux types de grains de mullite: des gros grains allongés et des petits grains équiaxes, ainsi que d'une dispersion de grains de zircone en sites intergranulaires. Celle de l'échantillon RS3 est composée uniquement de grains équiaxes de mullite et d'une dispersion de grains de zircone en sites intergranulaires, tandis que celle de l'echantillon RS2 est composée de grains de mullite de forme irrégulière et de grains de zircone arrondis, distribués en sites intra et intergranulaires. La composition de la mullite a été examinée en se basant sur la longueur du paramètre de maille c. Seule la mullite de l'échantillon RS2 semble présenter une composition en alumine plus élevée que 60% en

Journal of the European Ceramic Society 0955-2219/94/$7.00

moles mais se rapproche de cette valeur par un traitement de recuisson à 1570°C.

1 Introduction

Mullite is considered as a candidate for high-temperature engineering material because it shows good creep resistance, chemical stability, good fracture strength at high temperature and a low thermal expansion coefficient. Fracture toughness of mullite is, however, rather poor for these applications. Mullite-based composites with dispersal zirconia particles have been widely studied to overcome this disadvantage. Mullite–zirconia composites, therefore, have been prepared by the following various methods; (1) mechanical mixing of mullite and zirconia,[1–3] (2) mechanical mixing of alumina and zircon[4,5] and (3) sol–gel mixing of silica, alumina and zirconia.[6–8] Mullite–zirconia composites prepared by the sol–gel method show good fracture toughness and strength at room temperature. Although deterioration of high-temperature mechanical properties is considered by the addition of zirconia, no apparent lowering is reported.[8]

Various toughening mechanisms have been proposed to explain the role of zirconia particles; (1) stress-induced transformation toughening mechanism by zirconia in the crack-tip stress field,[4,6–8] (2) metastable solid-solution toughening mechanism,[2,3,9] and (3) microcrack toughening mechanism,[4,6–8,10] which is introduced due to the transformation of tetragonal zirconia to monoclinic phase.

In this paper, mullite–zirconia composites were prepared by three different routes and their formation reactions, sinterability and microstructures examined.

2 Experimental Procedures

2.1 Preparation of composites

Mullite–zirconia composites were prepared by three different kinds of combination of the starting materials; (1) MM sample: sintering of mechanically mixed mullite and zirconia powders; (2) RS2 sample: reaction-sintering of alumina and zircon powders, and (3) RS3 sample: reaction sintering of alumina, silica and zirconia powders. The starting powders used were mullite (MP-20, Chichibu Cement Co.), zirconia (NZP-0Y, Nissan Chemicals Co.), alumina (TM-DAR, Taimei Chemicals Co. and AKP-30, Sumitomo Chemicals Co.), zircon (Tosoh Co.)[11–14] and silica (Aerosil 200, Nippon Aerosil Co.). All of these powders were of high purity and small particle size.

In the reaction-sintering methods, the starting materials were mixed to give 60 mol% Al_2O_3, i.e. mullite composition (alumina/silica = 3/2). The content of zirconia was fixed to be 20 vol.% except for the RS2 sample, in which the content was 24 vol.%. The RS2 and RS3 samples were prepared using two different kinds of alumina powder and they were designated as the RS2(T) and RS3(T) for the samples using the TM-DAR alumina powder, and the RS2(A) and RS3(A) for the samples using the AKP-30 alumina powder.

All the mixtures were ball-milled with ethanol using YTZ balls in diameter of 2 mm and a plastic container. They were dried with stirring on a hot-stirrer and sieved through a 100 mesh nylon filter. Powder compacts were formed by a uniaxial press at 400 MPa. They were fired in air at various temperatures and duration times by heating and cooling rates at 15° and 30°/min, respectively. Apparent densities of the fired bodies were measured by a conventional Archimedes' method using distilled water. The fired bodies were polished and thermally etched to observe the microstructure by a scanning electron microscopy (SEM).

2.2 Characterization

The particle size distribution of the raw materials used was measured with a laser granulometer (Microtrack, Nikkiso Co.). Average particle sizes of the raw material powders were 1·46 μm in mullite, 0·38 μm in alumina (TM-DAR), 0·45 μm in alumina (AKP-30), 0·20 μm in zirconia (NZP-OY), 0·66 μm in zircon and 12 nm in silica (Aerosil 200). Here, the data of silica is quoted from the catalogue and that of zirconia was measured with a centrifugal sedimentation granulometer (SA-CP3, Shimazu Co.).

X-Ray diffraction experiments were performed with an X-ray powder diffractometer (Geigerflex, Rigaku Co.) using monochromated CuK_α radiation. Identification and semi-quantitative analysis of the crystalline phases were done on the polished fired-body samples. The reflections used for the semi-quantitative analysis were 111 and 11$\bar{1}$ for m-zirconia, 113 for alumina, 200 for zircon and 210 for mullite. The ratio of tetragonal zirconia (t-zirconia) was evaluated using Toraya's method.[15] Lattice parameters of mullite were calculated by the least-squares method using the powdered samples. Calculations were performed using 11 reflections, in which reflection angles were precisely measured using Si powder (NBS 640a) as an internal standard.

Shrinkage of the pressed samples was measured by a loadless dilatometer at a heating rate of 10°C/min. The samples used were formed to a

rectangular rod shape with 4 × 4 × 35 mm in size by an isostatic press at 100 MPa.

3 Results and Discussion

3.1 Thermal reaction

Figure 1 shows the ratio of the crystalline phases in the samples fired at various temperatures. In the RS2 samples, the following thermal reaction is expected at high temperature:

$$3Al_2O_3 + 2ZrSiO_4 \rightarrow 3Al_2O_3 \cdot 2SiO_2 + 2ZrO_2$$

This reaction largely proceeded between 1440 and 1480°C, and was completed at 1520°C when the finer alumina particles (TM-DAR) were used as the raw material. On the other hand, the decomposition reaction of zircon became sluggish when the coarser alumina powder (AKP-30) was used. This difference is caused by the particle size difference between the two alumina powders. The present result in the RS2 samples is compatible with the data reported by Boch *et al.*[16]

In the RS3 samples, formation of mullite occurred from a lower temperature than that in the RS2 samples. The reaction was completed by firing at 1480°C in the TM-DAR powder but at 1520°C in the AKP-30 powder. The difference between these two samples is considered to be similar to the RS2 samples. A small amount of zircon was formed from the reaction between silica and zirconia powders in the RS3 samples. It remained in the samples up to 1520°C and was rather higher temperature than that of alumina was expensed.

In the MM samples, a reverse reaction to form zircon occurred and its formation amount slowly increased as the firing temperatures increased up to 1520°C. Zircon in these samples would always be formed in the boundaries of mullite and zirconia, whereas in the RS3 samples its formation does not always follow the same route. Complete decomposition of zircon between 1520 and 1570°C in this study is compatible with the phase diagram reported by Toropov & Galakhov.[17]

3.2 Sinterability

Figure 2 shows the change of apparent density of the samples fired at various temperatures for 12 h against firing temperature. Relative densities are calculated for the obtained apparent densities against the theoretical densities of the samples, which were evaluated from the amount of each crystalline phase and the theoretical density. The theoretical density of each crystalline phase used for the calculation is as follows; 3·17 for mullite

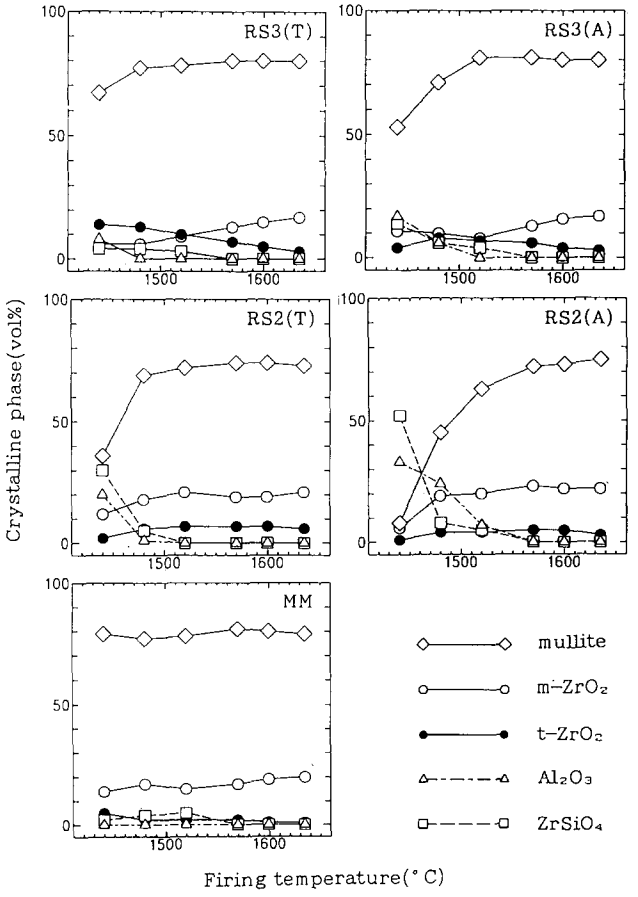

Fig. 1. Ratio of the crystalline phases in the samples from various raw materials fired at various temperatures (duration: 12 h).

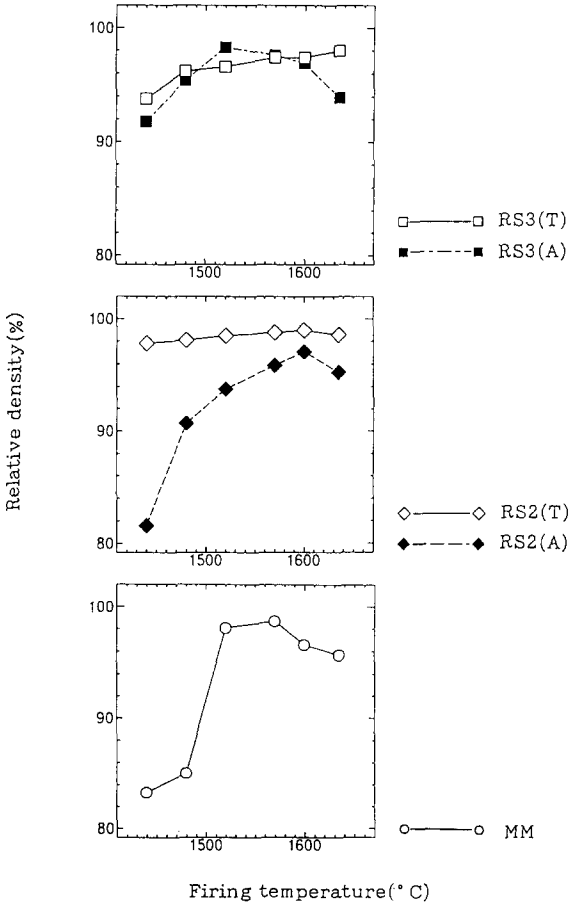

Fig. 2. Relative density of various samples as a function of firing temperature (duration: 12 h).

(JCPDS card #15–776), 4·67 for zircon (JCPDS card #6–0266), 5·86 for t-zirconia (JCPDS card #24–1164), 5·83 for m-zirconia (JCPDS card #13–307) and 3·99 g/cm^3 for alumina (JCPDS card #10–173). Since densification of mullite using this powder needs firing over 1600°C, addition of zirconia is found to lower the firing temperature.

The relative density of the MM sample increased as the firing temperature increased and reached to the maximum value at 1570°C As the firing temperature increased, the relative density again decreased.

All the relative densities of the RS3 samples were over 90% even for a firing temperature of 1440°C. They showed only a little change and maintained a high level between 1480 and 1635°C. Densification of these samples occurred at a much lower firing temperature than that of the MM samples. The shrinkage measurement of these samples revealed that the densification started as low as 1100°C, as shown in Fig. 3. It occurs by rearrangement of particles, due to a viscous flow mechanism of amorphous silica.

In the case of the RS2 samples, two samples using the different alumina powders showed quite different density curves against the firing temperature. The relative densities of the RS2(T) sample showed almost full density from the firing temperature at 1440°C and maintained it up to 1635°C. Considering the crystalline phase in the lower temperatures, as shown in Fig. 1, the densification of this sample occurred in the stage of zircon and alumina, and was corresponding to the stage before the thermal reaction of mullite and zirconia. On the other hand, the relative densities of the RS2(A) samples were very low compared with those of the RS2(T) samples. Large differences in the sinterability of the RS2(A) and RS2(T) samples was attributed to the difference of sinterability in the alumina powders used. In the case of the RS3 samples, enhancement of sinterability due to the viscous flow of amorphous silica masked the large difference of sinterability in the two alumina powders as a result.

3.3 Chemical composition of mullite

Figure 4 shows the relation between the length of lattice parameter of the *a*-axis and the firing temperature of three samples. Since the chemical composition of mullite can be evaluated from the lattice parameter of the *a*-axis, it is calculated using the relation reported by Ban & Okada.[18]

The lattice parameter of the *a*-axis of the MM sample fired at 1570°C was close to that of the JCPDS data (#15-776), and the chemical composition was calculated to be 60·7 mol% Al_2O_3. This value is just a little in excess of the alumina content compared with that of the catalogued data of the as-received mullite powder (60·2 mol% Al_2O_3). It may be due to the expense of small amount of silica by the transitional formation of zircon in the fired sample. As the firing temperature increased, the lattice parameter of the *a*-axis became a little longer, which means the chemical composition of mullite shifts to an alumina-rich composition. The phase diagram of the silica–alumina system reported by Prochazka & Klug[19] showed that the boundary line between mullite and liquid phase declined at high temperature towards an alumina-rich composition as the temperature increased. The variation of the lattice parameter of mullite in the MM sample was compatible with the phase diagram by Prochazka & Klug[19] and similar results were reported by Okada & Otsuka[20] and also Mizuno.[21]

Liberation of the silica component from the mullite and the formation of a liquid phase is considered above 1600°C when the bulk composition

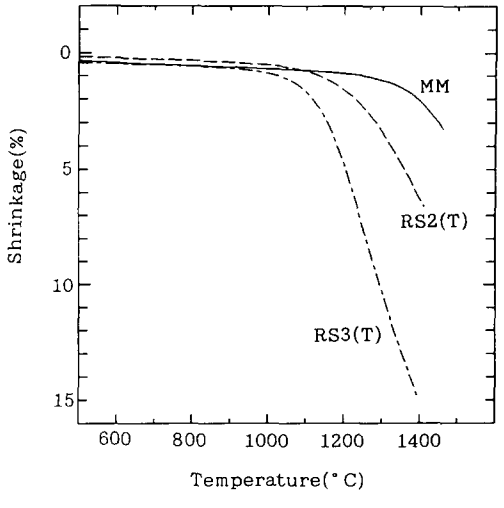

Fig. 3. Shrinkage curves of three samples against temperature.

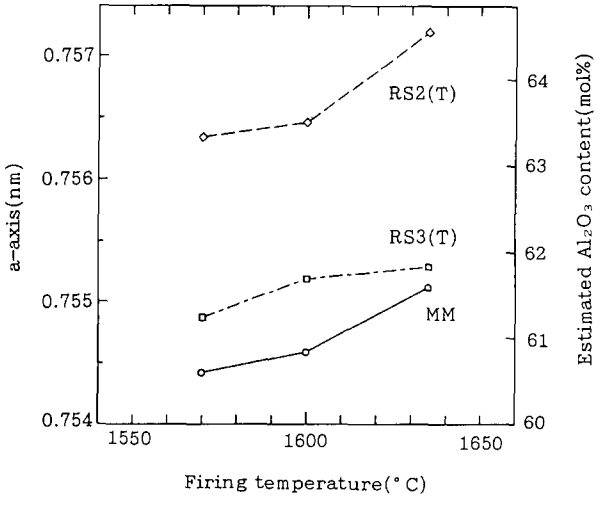

Fig. 4. Relation between the lattice parameter of the *a*-axis and the firing temperatures for three samples.

of the sample is around 60 mol% Al_2O_3. The liquid phase is considered to exist at the grain boundaries and will cause liquid-phase sintering. Mullite grains are well known to grow into an elongated shape when they coexist with liquid phase at high temperatures. Liquid-phase sintering is, therefore, considered in the MM sample from the following facts; (1) the densification curve of the MM sample shown in Fig. 2 is a typical pattern in liquid-phase sintering, and (2) elongated mullite grains are observed in the microstructure of the MM samples, as mentioned later in Section 3.4.

In the RS3 samples, the chemical composition of mullite formed at 1570°C was around 61·2 mol% Al_2O_3 and it shifted a little further towards an alumina-rich composition as the firing temperature increased. The chemical composition at 1635°C was 61·8 mol% Al_2O_3 and was rather close to the solid-solution limit of the alumina-rich side reported by Aksay & Pask.[22] A considerable amount of residual silica component should exist in the samples, especially in those fired at high temperature.

The length of the lattice parameter of the *a*-axis of mullite in all the RS2(T) samples prepared at various firing temperatures was remarkably long. This result may be related to the poor reactivity between zircon and alumina, as mentioned in Section 3.1. Yoshimura and coworkers[23–25] showed that mullite crystallized at lower temperature from the zirconia–mullite samples prepared by the rapidly quenched method had longer lattice parameters than those of mullite in 60 mol% Al_2O_3. By a further firing treatment, the lattice parameters changed and approached the ordinary values. They concluded from these results that mullite crystallized from disordered states, such as from a melt, shows a tendency to have a composition with an excess of alumina. Formation of alumina-rich mullite results in unreacted silica. Yoshimura *et al.*[25] observed by high-resolution TEM that small amorphous silica domains, about 10 nm in size, were dispersed intergranularly in the alumina-rich mullite grains.

Incorporation of zirconia in mullite is reported to be limited[3] because the ionic radius of Zr atom is too large to substitute in the mullite structure. Schneider[26] pointed out that zirconium incorporation into the mullite structure occurred through the occupation of the structural voids produced by oxygen vacancies evolved by charge compensation of $2Si^{4+} + O^{2-} \rightarrow 2Al^{3+} + \square$ substitution; however, it should be less than 1% even in 2/1-mullite. On the other hand, a considerable amount of zirconia incorporation was suggested in the transient state of mullite–zirconia samples by Yoshimura and coworkers.[23–25] Incorporation of zirconia in mullite can be estimated using the relation between the lattice parameter of the *a*-axis and the cell volume, which is originally reported from the incorporation of titania and/or iron oxide components by Cameron[27] and later modified for zirconia by Yoshimura and coworkers.[24,25] Figure 5 shows the relation between the lattice parameter of the *a*-axis and the cell volume of mullites. The data obtained for the RS2(T) sample fired at 1635°C for 12 h deviate from the line of mullite in the pure alumina–silica system. Using the estimation method of Yoshimura and coworkers,[24,25] the content of zirconia in this mullite was estimated to be 1 wt% and the composition of mullite was 64·3 mol% Al_2O_3. Then, this sample was annealed at 1570°C for 12, 72 and 144 h. As shown in Fig. 5, the length of the *a*-axis and the cell volume were found to be decreased by the annealing. The chemical composition of their mullites can be estimated similarly. The chemical composition of mullite in the 12 h annealed sample was 63·6 mol% Al_2O_3 but the ZrO_2 content was reduced to less than 0·1 wt% ZrO_2. Those of the 72 and 144 h annealed samples were 62·7 and 62·2 mol% Al_2O_3, respectively. No ZrO_2 incorporation was considered in these samples. The chemical composition of mullite in these samples approached those obtained in the RS3(T) and MM samples. Zirconia was considered to incorporate only in the transient state of mullite as in the case of the RS2 samples and did not incorporate in the RS3 and MM samples. Therefore, mullite formed by the thermal reaction of (zircon+alumina) was via a somewhat different formation route from the other mullites.

3.4 Microstructure

Microstructures of three samples fired at 1570 and 1615°C for 6 h are shown in Fig. 6. Among these,

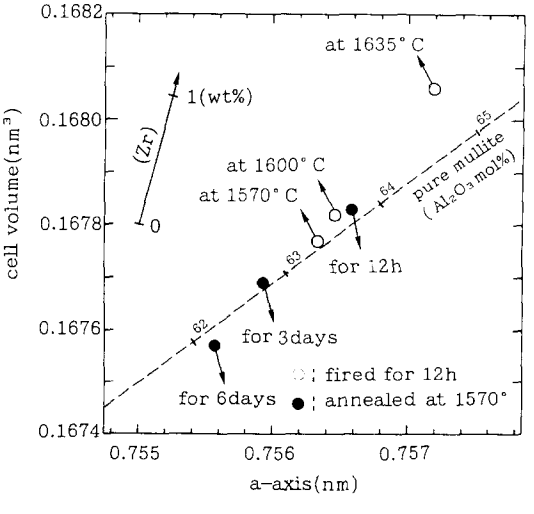

Fig. 5. Effect of annealing for the RS2(T) samples on the relation between the *a*-axis and the cell volume of mullite.

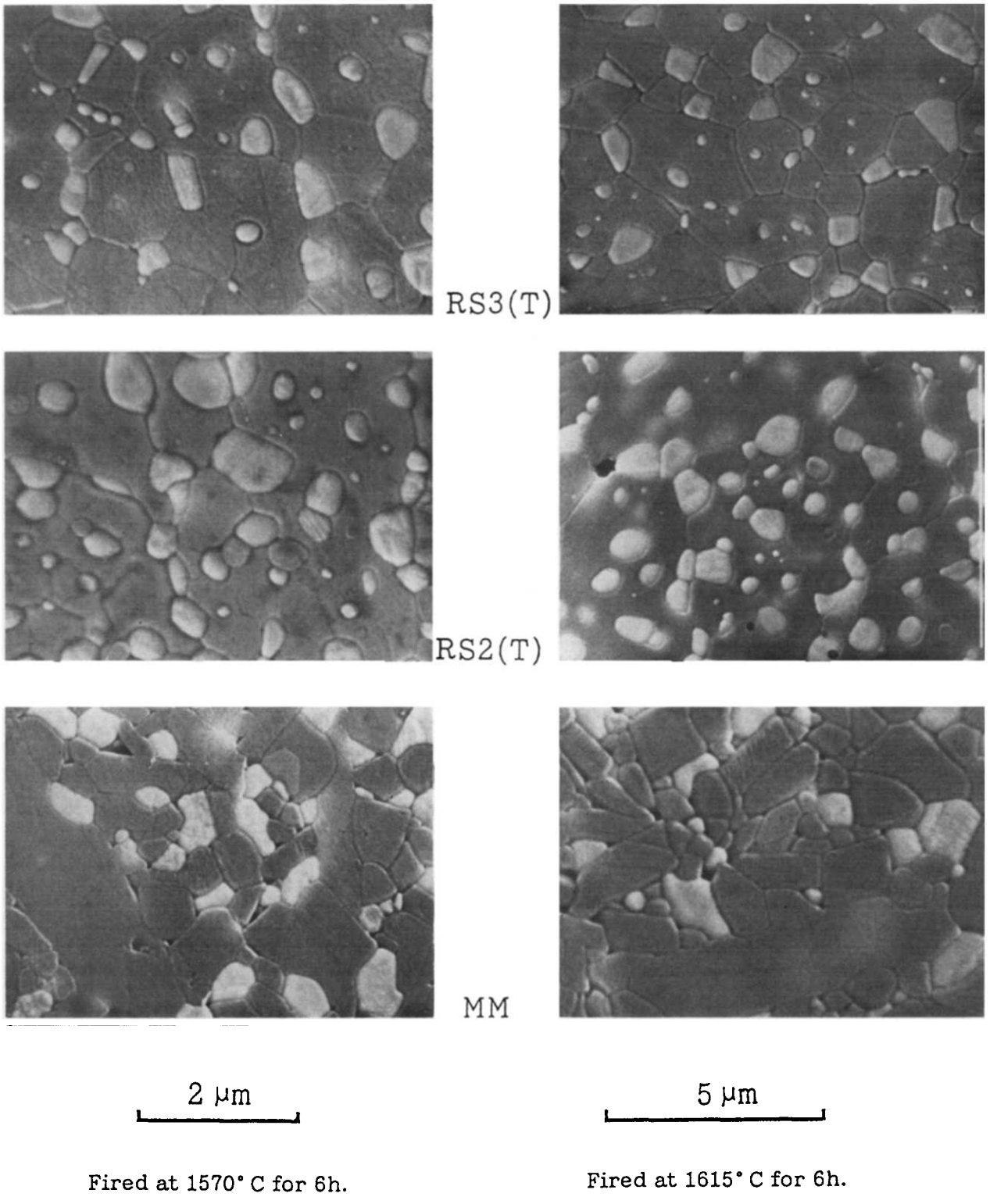

Fig. 6. SEM photographs of polished and thermally etched surface of the samples fired at 1570 and 1615°C.

the microstructures of the MM samples apparently differed from those of the RS2 and RS3 samples. Mullite in the MM samples clearly showed grain growth and a part of the mullite grains became an elongated shape as the firing temperature increased. The grain size of zirconia as well as mullite increased. Liberation of silica from mullite and formation of liquid phase at firing temperatures above 1600°C are considered to be the main reason for this microstructure.

On the other hand, the microstructures of the RS2 and RS3 samples did not show such an exaggerated grain growth. This result suggests that there is a certain relation between the existence of exaggeratedly grown mullite grain and lowering of the relative density of the fired bodies at higher temperature. Mullite in the RS3 samples was an equiaxed shape and was a typical shape observed in alumina-rich mullite. The results in the SEM observation are compatible with that of the chem-

ical composition of mullite as shown in Fig. 4. Zirconia grains in these samples were distributed mostly intergranularly and only a small part of them were distributed intragranularly. The shape of intergranularly distributed zirconia grains became somewhat angular as the firing temperature increased.

On the other hand, the microstructure of the RS2 samples was composed of irregularly shaped large mullite grains and round-shaped zirconia grains, which were distributed both intergranularly and intragranularly. The ratio of intragranular zirconia grains was higher in the RS2 samples than in the RS3 samples. The change of the microstructure against the firing temperature was smallest in the RS2 samples among the three samples. Round-shaped zirconia grains were one of the characteristic points of this microstructure. Since Wallace *et al.*[28] reported that the existence of the round-shaped zirconia grains in the zirconia–mullite composites is evidence of the formation of 'non-crystalline mullite phase', and zirconia particles were not allowed to form facets in that phase, formation of the similar phase was considered as a transient state of the RS2 samples. Yoshimura *et al.*[25] found nano-sized amorphous silica particles in the interior of alumina-rich mullite grains in the rapidly quenched samples. In the SEM photograph of the RS2 sample, very small particles with a different contrast to zirconia particles were found, as indicated by the arrows in Fig. 7. These particles may be similar to the ones reported by Yoshimura *et al.*[25] Such particles should be formed as a residual phase by the formation of extraordinarily alumina-rich mullite phase in the RS2 samples. Further study by a TEM is necessary to clear up this uncertainty observed in the RS2 samples.

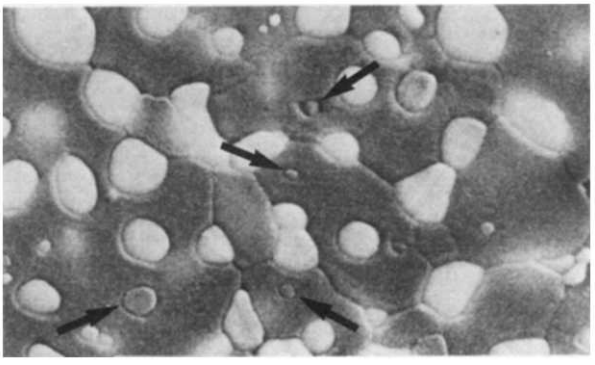

Fig. 7. SEM photograph showing unidentified particles in the RS2 samples.

4 Conclusions

Mullite–zirconia composites were prepared from three kinds of combination of the starting materials and their phase formation reaction, sinterability and microstructure investigated. The following conclusions can be drawn.

(1) The mixture of mullite and zirconia powders (MM): Sinterability of this sample was not so good compared with the others. At higher temperature, it released silica from mullite and formed a liquid phase, which caused the growth of elongated large mullite grains in the microstructure.

(2) The mixture of alumina, amorphous silica and zirconia powders (RS3): Sinterability of this sample was good because of the enhancement of densification by a viscous flow mechanism due to amorphous silica phase. Equiaxed mullite grains and intergranularly dispersed zirconia grains formed the microstructure.

(3) The mixture of alumina and zircon (RS2): Extremely alumina-rich mullite were formed transiently in this sample. Their microstructures were composed of irregularly shaped mullite and intra/intergranularly dispersed zirconia grains. Some extent of Zr atoms was considered to be incorporated in the transient state mullite.

Acknowledgement

The authors are grateful to Mr T Mori of the Tosoh Company for supplying the zircon samples.

References

1. Prochazka, S., Wallace, J. S. & Claussen, N., Microstructure of sintered mullite–zirconia composites. *J. Am. Ceram. Soc.*, **66** (1983) c125–7.
2. Claussen, N. & Jahn, J., Mechanical properties of sintered in-situ reacted mullite–zirconia composites. *J. Am. Ceram. Soc.*, **63** (1980) 228–9.
3. Moya, J. S. & Osendi, M. I., Microstructure and mechanical properties of mullite/ZrO_2 composites. *J. Mater. Sci.*, **19** (1984) 2909–14.
4. Ismail, M. G. M. U., Nakai, Z. & Somiya, S., Properties of zirconia-toughened mullite synthesized by the sol–gel method. *Adv. Ceram.*, **24** (1988) 119–26.
5. Rundgren, K., Elfving, P., Tabata, H., Kanzaki, S. & Pompe, R., Microstructures and mechanical properties of mullite–zirconia composites made from inorganic sols and salts. *Ceram. Trans.*, **6** (1990) 553–66.
6. Claussen, N. & Wallace, J. S., Comment on 'Reply to "Mechanical properties of sintered in-situ reacted mullite– zirconia composites"'. *J. Am. Ceram. Soc.*, **64** (1981) c79–80.
7. Kubota, Y. & Takagi, H., Preparation and mechanical properties of mullite–zirconia composites. *Adv. Ceram.*, **24** (1988) 999–1005.
8. Osendi, M. I., Miranzo, P. & Moya, J. S., Solid-solution

effects on the fracture toughness of mullite–ZrO_2 composites. *J. Mater. Sci. Lett.*, **4** (1985) 1026–8.
9. Moya, J. S. & Osendi, M. I., Effect of ZrO_2 (ss) in mullite on sintering and mechanical properties of mullite/ZrO_2 composites. *J. Mater. Sci. Lett.*, **2** (1983) 599–601.
10. Leriche, A., Deleter, M. & Cambier, F., Relations among microstructure and mechanical properties in reaction-sintered mullite–zirconia composites. *Adv. Ceram.*, **24** (1988) 1083–9.
11. Kobayashi, H., Takano, T., Mori, T., Yamamura, H. & Mitamura, T., Preparation of $ZrSiO_4$ powder using sol–gel process (Part 1)—influence of starting materials and seeding. *J. Ceram. Soc. Jpn.*, **98** (1990) 567–72.
12. Kobayashi, H., Takano, T., Mori, T., Yamamura, H. & Mitamura, T., Preparation of $ZrSiO_4$ powder using sol–gel process (Part 2)—preparation conditions of $ZrSiO_4$ composition precursor gels. *J. Ceram. Soc. Jpn*, **98** (1990) 1109–13.
13. Kobayashi, H., Terasaki, T., Mori, T., Yamamura, H. & Mitamura, T., Preparation of $ZrSiO_4$ powder using sol–gel process (Part 3)—preparation conditions of $ZrSiO_4$ composition precursor gels from $Si(OC_2H_5)_4$ and $Zr(O^iC_3H_7)_4$ alkoxides. *J. Ceram. Soc. Jpn*, **99** (1991) 42–6.
14. Mori, T., Hoshino, H., Ishikawa, Y., Yamagichi, T., Yamamura, H., Kobayashi, H. & Mitamura, T., Preparation of $ZrSiO_4$ powder using sol–gel process (Part 4)—preparation from $ZrOCl_2$ and SiO_2. *J. Ceram. Soc. Jpn*, **99** (1991) 227–32.
15. Toraya, H., Yoshimura, M. & Somiya, S., Calibration curve for quantitative analysis of the monoclinic–tetragonal ZrO_2 system by X-ray diffraction. *J. Am. Ceram. Soc.*, **67** (1984) c119–21.
16. Boch, P., Chartier, T. & Giry, J. P., Zirconia-toughened mullite/The role of zircon dissociated. *Ceram. Trans.*, **6** (1990) 473–94.
17. Toropov, N. A. & Galakhov, F. Ya, In *Phase Diagrams for Ceramics*, ed. M. K. Reser. The American Ceramics Society, OH, USA, 1969, Fig. 362.
18. Ban, T. & Okada, K., Structure refinement of mullite by the Rietveld method and a new method for estimation of chemical composition. *J. Am. Ceram. Soc.*, **75** (1992) 227–30.
19. Prochazka, S. & Klug, F. J., Infrared-transparent mullite ceramic. *J. Am. Ceram. Soc.*, **66** (1983) 874–80.
20. Okada, K. & Otsuka, N., Chemical composition change of mullite during formation process. *Sci. Ceram.*, **14** (1988) 497–502.
21. Mizuno, M., Microstructure, microchemistry, and flexural strength of mullite ceramics. *J. Am. Ceram. Soc.*, **74** (1991) 3017–22.
22. Aksay, I. A. & Pask, J. A., Stable and metastable equilibria in the system SiO_2–Al_2O_3. *J. Am. Ceram. Soc.*, **58** (1975) 507–12.
23. Yoshimura, M., Kaneko, M. & Somiya, S., Crystallization of mullite–zirconia amorphous materials prepared by rapid quenching. *Yogyo-Kyokai-Shi*, **95** (1987) 64–70.
24. Yoshimura, M., Kaneko, M., Hanaue, Y. & Somiya, S., Mullite–ZrO_2 ceramics from rapidly quenched ZrO_2–SiO_2–Al_2O_3 amorphous phase. *Adv. Ceram.*, **24** (1988) 1053–62.
25. Yoshimura, M., Hanaue, Y. & Somiya, S., Non-stoichiometric mullites from Al_2O_3–SiO_2–ZrO_2 amorphous materials by rapid quenching. *Ceram. Trans.*, **6** (1990) 449–56.
26. Schneider, H., Zirconium incorporation in mullite. *N. Jb. Miner. Mh.*, **1986** (1986) 172–80.
27. Cameron, W. E., Composition and cell dimensions of mullite. *Ceram. Bull.*, **56** (1977) 1003–11.
28. Wallace, J. S., Petzow, G. & Claussen, N., Microstructure and property development of in-situ reacted mullite–ZrO_2 composites. *Adv. Ceram.*, **12** (1984) 436–42.